Chemical Engineering Science 66 (2011) 2232–2240

Contents lists available at ScienceDirect

Chemical Engineering Science

journal homepage: www.elsevier.com/locate/ces

Reaction kinetics and producer gas compositions of steam gasification of coal and biomass blend chars, part 2: Mathematical modelling and model validation

Qixiang Xu [a], Shusheng Pang [a,*], Tana Levi [b]

[a] Department of Chemical and Process Engineering, University of Canterbury, New Zealand
[b] CRL Energy Ltd., Wellington, New Zealand

ARTICLE INFO

Article history:
Received 5 October 2010
Received in revised form
27 January 2011
Accepted 23 February 2011
Available online 3 March 2011

Keywords:
Co-gasification
Blended biomass and coal
Solid char
Producer gas
Gasification reactions
Reactions kinetics

ABSTRACT

In gasification of biomass, coal and blended biomass and coal, there are two steps including an initial pyrolysis process followed by gasification of solid char. The latter process is a slow process and thus dominates the whole gasification. In our previous paper (Xu et al., in press), the differences between steam gasification of biomass chars and that of coal chars have experimentally been investigated and the results show that these differences are mainly due to the difference in microstructures of these two fuels. In this work, a mathematical model of char gasification is developed based on reaction kinetics and gas transportation of both the producer gas and the gasification agent (steam). The model also includes mass conservation equations for each of the gas components and solid carbon involved in the gasification process. This has resulted in a set of highly nonlinear differential equations which have been solved using a numerical technique to predict gas production rate, gas compositions and carbon consumption rate during the gasification.

The developed mathematical model is validated using experimental results reported in previous paper (Xu et al., in press), and close agreement between the simulation results and the experimental values have been observed. From the modelling, it has been confirmed that the char gasification is mainly determined by the characteristics of char matrix including the exposed surface area and the micro-pore size. The former determines intrinsic reaction rate and the latter influences the intra-particle mass transportation. Biomass char has more amorphous structure, thus the intrinsic reaction rate is enhanced. For coal char, the larger pore size enables the high transport rate of the gasification agent (water vapour) into the char particles but the resultant gases have higher resistance to transfer through compact clusters. For simulation of the blended biomass and coal, the blend properties were determined based on the blend proportion of each fuel. The close agreement between the simulation results and experimental data suggests that the approach in this work can adequately quantify the gasification kinetics and the gas composition.

1. Introduction

The process of solid fuel gasification within a fluidized bed reactor can be divided into two main steps after the initial short drying: (1) fast pyrolysis of the raw materials and (2) subsequent gasification of resultant chars. The former is a short process generating solid char and volatile gases. The latter consists of a series of heterogeneous reactions of the chars with gasification agent (air, oxygen or steam), and reactions among reactant and resultant gases. The char gasification process is a much slower conversion process compared to the initial pyrolysis thus it is dominant in the whole gasification process (Marcio, 2004; Everson et al., 2006). Therefore, fundamental understanding and quantification of the char gasification are crucial for optimisation of whole gasification process and for design of the gasifier.

The reaction kinetics in gasification of the chars has been widely studied in the last few decades. From the previous paper by the authors (Xu et al., in press), it was found that both the biomass char and the coal char are porous in structure and mainly consist of carbon element. The distinct differences in physical and chemical properties of the biomass chars and the coal chars result in different gasification characteristics (Lu et al., 2002; Sadhukhan et al., 2009; Xu et al., in press). Compared with coal char, the biomass char has lower density and is structurally more amorphous (Klose and Wolki, 2004; Xu et al., in press). Due to the differences in the microstructure and gas reaction kinetics, the overall reaction can

* Corresponding author.
E-mail address: shusheng.pang@canterbury.ac.nz (S. Pang).

0009-2509/$ - see front matter © 2011 Elsevier Ltd. All rights reserved.
doi:10.1016/j.ces.2011.02.054

be influenced by the intrinsic reaction rate and transportation of gases involved (Gupta and Saha, 2003). The rate of heterogeneous reactions, which take place on the contact surface of solid and reactant gas, are dominated by the inner surface area of the pores (Bhatia and Perlmutter, 1980). The diameter of the pores also influences the transportation of the reactant gases into the solid and the resultant gases out of the solid (Krishna and Wesselingh, 1997). Therefore, the gasification rate is dominated by chemical reactions involved and the rate of mass transfer which is, in turn, affected by the char structure.

Due to the small diameter of chars in the order of millimetres, a gas concentration gradient exists within the particle and, therefore, a lump model is inadequate to simulate the char gasification process (Wang and Bhatia, 2001). A dynamic model is, on the other hand, desirable for quantifying the char gasification characteristics under different operating conditions. Biggs and Agarwal (1997) developed a one-dimensional model to simulate char particle in oxygen in which reactions and gas diffusion were considered and the products compositions were predicted at different operation conditions. In a separate study, Wang and Bhatia (2001) proposed a similar combustion model to investigate the structure evolution and fragmentation of the chars. Recently, Yamashita and his colleagues (Yamashita et al., 2006) developed a three dimensional model to simulate the structure evolution of the cubic shape char particle in the oxygen gasification. However, the dynamic model for simulation of steam gasification has not been found in literature. In addition, the existing models are all for a single fuel thus there is an apparent gap in modelling of co-gasification or co-combustion of two different fuels which have different properties (such as biomass and coal). Furthermore, in understanding of the co-gasification process of blended coal and biomass, the reactivity of the blend chars has been reported to have a synergetic effect and the simple additive rule could not be applied to predict the gasification behaviour. The single particle model based on fundamental physical and chemical phenomena will also be useful to quantify the gasification process.

In the previous study (Xu et al., in press), a series of gasification tests were performed in order to experimentally investigate the gasification process and to understand gasification mechanism. From this study, it has been concluded that the biomass char has larger intrinsic reactivity while coal char has better effective mass permeability. The objectives of the current work are to develop a dynamic mathematical mode for the char gasification and to validate the developed model using the experimental results reported previously by the authors (Xu et al., in press). In the char gasification, steam is used as the gasification agent and the chars include biomass char, coal char and chars of blended biomass and coal. From the developed model, the influence of structure difference on the gasification characterises will be examined and reasons for the differences in gasification performance of the different types of chars will be investigated.

2. Development of a mathematical model for steam gasification of chars

2.1. Transfer process for reactant and resultant gases in a solid char

In gasification, although the chemical reactions between gasification agent (steam) and carbonaceous materials are the same for both the biomass char and the coal char, the physical and the structural properties among these two types of chars are significantly different which result in very different characteristics exhibited in the gasification process. The gasification is a complicated process consisting of both physical and chemical processes within a char particle: (1) gasification agent diffusion from bulk gas into the particle through the micro-pores, (2) chemical reactions among gases, and between gas and char matrix, and (3) resultant gases moving out from the char particle by diffusion and bulk flow through the micro-pores. The above processes can be illustrated in a schematic diagram as shown in Fig. 1.

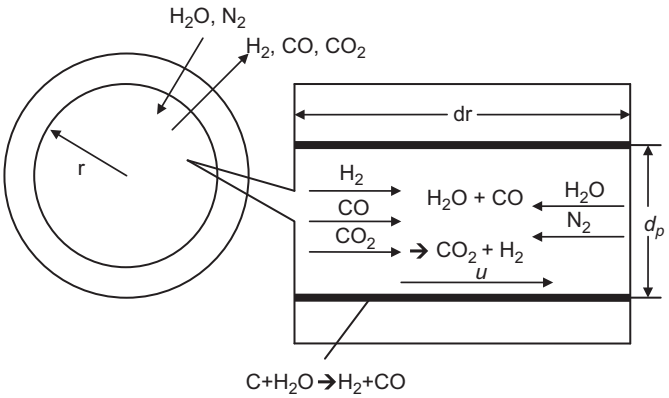

Fig. 1. Schematic diagram of steam gasification of a single char particle. d_r is the infinitesimal length in radius direction of the char particle and d_p is the diameter of the micro-pore.

2.2. Mass balance equations in a spherical coordinate

The modelling of steam gasification of a single char particle includes mass balances of all matters involved, transportation of gas phase reactants and products, reaction kinetics of the gases and the char over an infinitesimal volume with the diameter increment, d_r. In the development of the gasification model, it is assumed that all the macro-char particles are regular spheres with the same initial size and micro-pore diameter. This assumption is valid from the observation that after char generation, the char particles are generally no longer cylindrical in spite of the cylindrical pellets used for making chars. During the char generation, the internal structure of solid changes and the original pellets are fragmentized into several smaller sized pieces due to outward volatile fluxes. Furthermore, in the fluidized bed, the relative motion between solid and gas phases will enhance such fragmentation process. The highly non-spherical chars are much more fragile, so that smaller and more spherical particles are formed.

Other assumptions in the model include:

- For the small and spherical char particles, all deviation variables are only the functions of time (t) and distance in radius (r). This assumption is tenable for a fluidized bed reactor because the gases flow through the char bed with high velocity and the variation in gas composition and gas film mass transfer coefficient outside the char particles are the minimum.
- The mass transfer occurs through convection and diffusion within the char particle.
- Due to the small size of the particle, it is assumed that the char particle has a uniform temperature distribution.
- Three chemical reactions occurring in the char gasification are considered, these are:

Steam Gasification Reaction: $H_2O+C\rightarrow H_2+CO$ (1)

Water–Gas Shift Reaction: $H_2O+CO\leftrightarrow H_2+CO_2$ (2)

Bouduard Reaction: $CO_2+C\rightarrow 2CO$ (3)

Therefore, the resultant gases from the char gasification are H_2, CO and CO_2.

In the model, the independent variables involved are: (1) molar concentration of the gaseous species of H_2O (gasification agent), H_2, CO, CO_2 and N_2 (carrier gas), nominated as C_i, $i=1$ to 5 and (2) conversion rate of solid char represented by X_s which is defined in the previous paper of the authors (Xu et al., in press).

Based on the isothermal assumption, only mass balance calculations are needed in the model which is derived as follows:

$$\frac{\partial(\Phi C_i)}{\partial t}+\frac{1}{r^2}\frac{1}{\partial r}(r^2N_i)=\sum_{j=1}^{3}v_{ij}R_j \tag{4}$$

where Φ is the porosity of the char structure; N_i the net mass flux of ith component, $i=1, 2,\ldots,5$; v_{ij} the stoichiometric coefficient of ith component in jth reaction; R_j the intrinsic reaction rate of the jth reaction as given in Eqs. (1)–(3).

Using the matrix form, the above mass conservation equation of all gas species can be expressed as

$$\frac{\partial(\Phi\mathbf{C})}{\partial t}+\frac{1}{r^2}\frac{1}{\partial r}(r^2\mathbf{N})=\mathbf{vR} \tag{5}$$

In which **C** is the vector of gas component concentration with 5 rows,

$$\mathbf{C}=\begin{bmatrix}C_1\\C_2\\C_3\\C_4\\C_5\end{bmatrix}$$

N is the vector of gas component net fluxes, also of 5 rows. **R** is the vector of intrinsic rates of all reactions with 3 columns. **v** is the matrix of stoichiometric coefficients with 5×3 elements

$$\mathbf{v}=\begin{bmatrix}-1&-1&0\\1&1&0\\1&-1&2\\0&1&-1\\0&0&0\end{bmatrix}$$

Initial and boundary conditions for Eq. (5) are:

$$\frac{\partial\mathbf{C}}{\partial t}=0 \quad \text{at } r=0$$
$$\mathbf{C}=\mathbf{C}_s \text{ at } r=r_a \tag{6}$$

Here $\mathbf{C}_s$ is the concentration of a gas species on the apparent surface of the particle.

The net flux vector **(N)** is the sum of the diffusion and the convection of the bulk gas in the porous structure within the char particle:

$$\mathbf{N}=\mathbf{J}+u\mathbf{C}=-\frac{\Phi}{\tau}(D_{eff}\nabla\mathbf{C}+u\mathbf{C}) \tag{7}$$

where **J** is the diffusion flux vector of gas components; u is the linear gas velocity of the bulk gas phase; τ is the tortuosity of the pores which is unity ($\tau=1$) for cylindrical shaped pores; and D_{eff} is the effective diffusivity of the gas components in the char matrix.

2.3. Transportation of gas molecules in the char matrix

For diffusion of gas species in porous structure, if the length of mean free path of the gas molecules is larger than the micro-pore diameter, the collision between the gas molecules and the pore wall becomes more frequent and the overall diffusivity of the gas in the solid structure is reduced due to the restriction of the molecule transportation by the narrow space within the pore. This phenomenon is well known as Knudsen Diffusion. In this model, the mean pore diameter is in the order of a micrometre which is significantly less than the mean free path of gas molecules corresponding to the gasification temperatures investigated. Therefore, determination of diffusivity of gas components in the char needs to take into account the effect of both diffusion and convective bulk flow. The diffusion of ith gas component in the char matrix could be evaluated by dusty-gas model which implements the Knudsen Diffusivity into the Maxwell–Stephan multi-component diffusion model. On the other hand, viscous flow occurs under the pressure gradient within the pores which also contributes to the overall flux of a given gas component. Under normal pressure conditions the relationship among species flux, species concentration and pressure gradient acting on the ith gas component can be described by the following equation (Krishna and Wesselingh, 1997):

$$-\left(\nabla C_i+\frac{B_0}{D_{iK}\mu}C_i\nabla P\right)=\sum_{j=1}^{n}\frac{y_jN_i-y_iN_j}{D_{ij}^e}+\frac{N_i}{D_{iK}^e},\quad i=1,2,\ldots,n \tag{8}$$

where D_{ij}^e and D_{iK}^e are, respectively, the effective gas phase diffusivity and Knudsen Diffusivity in the porous material:

$$D_{ij}^e=\frac{\Phi}{\tau}D_{ij},\quad D_{iK}^e=\frac{\Phi}{\tau}D_{iK} \tag{9}$$

By applying the Ideal Gas Law, the following equations can be derived:

$$\nabla P=RT\nabla C_t \tag{10}$$

$$C_t=\sum_{i=1}^{n}C_i \tag{11}$$

Eq. (8) can also be expressed in a matrix form:

$$-\frac{\Phi}{\tau}\left(\nabla\mathbf{C}+\frac{RTB_0}{\mu}\nabla C_t[\mathbf{A}]\mathbf{C}\right)=[\mathbf{B}]\mathbf{N} \tag{12}$$

By re-arranging the above equation, the molar flux of gas components (**N**) can be determined by

$$\mathbf{N}=-\frac{\Phi}{\tau}\left([\mathbf{B}]^{-1}\nabla\mathbf{C}+\frac{RTB_0}{\mu}\nabla C_t[\mathbf{B}]^{-1}[\mathbf{A}]\mathbf{C}\right) \tag{13}$$

Substituting Eq. (13) into Eq. (5), the mass balance for gas components becomes:

$$\frac{\partial(\Phi\mathbf{C})}{\partial t}=\frac{1}{r^2}\frac{1}{\partial r}\left[r^2\frac{\Phi}{\tau}\left([\mathbf{B}]^{-1}\frac{\partial\mathbf{C}}{\partial r}+\frac{RTB_0}{\mu}\frac{\partial C_t}{\partial r}[\mathbf{B}]^{-1}[\mathbf{A}]\mathbf{C}\right)\right]+\mathbf{vR} \tag{14}$$

In the above equation, **[A]** and **[B]** are 5-dimensional square matrices. Their diagonal and off-diagonal elements are calculated by

$$A_{ii}=\frac{1}{D_{iK}} \tag{15}$$

$$A_{ij}=0 \tag{16}$$

$$B_{ii}=\frac{1}{D_{iK}}+\sum_{\substack{j=1\\j\neq i}}^{n}\frac{y_j}{D_{ij}} \tag{17}$$

$$B_{ij}=-\frac{y_i}{D_{ij}},\quad i=1,\ldots,5 \tag{18}$$

The Knudsen Diffusion coefficient of ith component in the pore, D_{iK}, is calculated by (Jackson, 1977):

$$D_{iK}=\frac{d_p}{3}\sqrt{\frac{8RT}{\pi M_i}} \tag{19}$$

where d_p is the mean diameter of pores.

The binary diffusion coefficient of component (D_{ij}) for species i in reaction j is estimated by correlation of Hirschfelder

(Welty et al., 1969):

$$D_{ij}=\frac{0.001858T^{3/2}\sqrt{(1/M_i)+(1/M_j)}}{P\sigma_{ij}^2\Omega_D} \tag{20}$$

In which M_i and M_j are the molecular weight of component i and j, respectively.

In Eq. (14), B_0 is the gas permeability of the porous char particle. With laminar gas flow in a cylindrical pore, B_0 can be evaluated by using the Hagen–Poiseuille equation:

$$B_0=\frac{d_p^2}{32} \tag{21}$$

The gas mixture viscosity in Eq. (14) can be evaluated by Wilke's correlation (Welty et al., 1969):

$$\mu=\sum_{i=1}^{n}\frac{y_i\mu_i}{\sum y_i\phi_{ij}} \tag{22}$$

$$\phi_{ij}=\frac{1}{\sqrt{8}}\left(1+\frac{M_i}{M_j}\right)^{-1/2}\left[1+\left(\frac{\mu_i}{\mu_j}\right)^{1/2}\left(\frac{M_j}{M_i}\right)^{1/4}\right]^2 \tag{23}$$

However, for the single gas species, the viscosity of ith component is determined by Sutherland's formula (White, 1991):

$$\mu_i=\mu_{0,i}\left(\frac{T_{0,i}+c_i}{T+c_i}\right)\left(\frac{T}{T_{0,i}}\right)^{3/2} \tag{24}$$

where $T_{0,i}$ is the reference temperature, $\mu_{0,i}$ is the reference viscosity at reference temperature, and c_i is the Sutherland's constant.

2.4. Gasification reaction kinetics

In this model, the three main reactions considered are expressed in Eqs. (1)–(3) and illustrated in Fig. 1. Among the three reactions, the Water–Gas Shift Reaction (Eq. (2)) is the gas phase homogeneous reaction within the void space of the char pores for conversion of H_2O and CO to CO_2 and H_2, the kinetics of this reaction is expressed as

$$R_2=k_2\left(C_1C_3-\frac{C_2C_4}{K_2}\right)\Phi=k_{0,2}e^{-E_{A,2}/RT}\left(C_1C_3-\frac{C_2C_4}{K_{0,2}e^{-\Delta G_2/RT}}\right)\Phi \tag{25}$$

where k_2 is the reaction kinetic constant, K_2 is the equilibrium constant, and $k_{0,2}$ and $K_{0,2}$ are, respectively, the pre-exponential factors. $E_{A,2}$ is the activation energy and ΔG_2 is the Gibbs free energy of the reaction.

The intrinsic rates of the other two heterogeneous reactions of the char gasification are dependent on temperature, concentration of the gasification agent (steam) and the activated reaction surface area of the solid. In general, kinetic models for intrinsic rates of heterogeneous reactions can be expressed as the product of three affecting parameters (Fermoso et al., 2008):

$$R_i=k(T)\,f(C)\,S(X) \tag{26}$$

In which k is the apparent rate constant which can be considered as a unique function of temperature, T, and is usually expressed in Arrhenius equation:

$$k(T)=k_{0,j}e^{-E_{A,j}/RT},\quad j=1,2,3 \tag{27}$$

where k_0 and $E_{A,j}$ are the pre-exponential factor and the activation energy, respectively.

The gas component function in Eq. (26), $f(C)$, represents the effect of the gas concentration on the reaction rate. For the reaction between steam and carbonaceous material, it can be expressed by the Langmuir type formulation. However in this model, it will be simplified to be $f(C)=C$, since the system was operated at atmospheric pressure, at which the intrinsic rate is linearly related to the concentration of gasification agent.

The specific reactive surface area evolution function in Eq. (26), $S(X)$, describes the change of the geometrical property of the solid char as the gasification proceeds. In the initial stage of the gasification process, the total surface area increases due to the size increase of the char pores during the initial heat-up period. After the initial stage, the pores contract and char particle size is reduced which causes the reduction of total surface area. Therefore, the random pore model, which contains competing effect of single pore size increase and destruction of overlapping region on the total surface area, is implemented to determine the surface area evolution (Bhatia and Perlmutter, 1980):

$$S(X)=S_0(1-X_s)\sqrt{1-\psi\ln(1-X_s)} \tag{28}$$

where S_0 is the specific surface area of char at $X_s=0$. ψ is the dimensionless parameter indicating the nature of pore structure:

$$\psi=\frac{4\pi L_0(1-\Phi_0)}{S_0^2} \tag{29}$$

In the above equation, L_0, S_0 and Φ_0 represent the initial pore surface, pore length and solid porosity, respectively (Bhatia, 1987). The value of parameter ψ is mainly dependent on the type of the solid fuel and the char formation condition (Mastsumoto et al., 2009; Sadhukhan et al., 2009).

Combining all of three reaction parameters, $k(T)$, $f(C)$ and $S(X)$, the complete form of the intrinsic reaction rate vector becomes:

$$R=\begin{pmatrix}R_1\\R_2\\R_3\end{pmatrix}=\begin{pmatrix}k_{0,1}e^{-E_{A,1}/RT}S_0(1-X_s)\sqrt{1-\psi\ln(1-X_s)}C_1\\k_{0,2}e^{-E_{A,2}/RT}\left(C_1C_3-\frac{C_2C_4}{K_{2,0}e^{-\Delta G_2/RT}}\right)[\Phi_0+(1-\Phi_0)X_s]\\k_{0,3}e^{-E_{A,3}/RT}S_0(1-X_s)\sqrt{1-\psi\ln(1-X_s)}C_4\end{pmatrix} \tag{30}$$

2.5. Char structural evolution

The local conversion of char is evaluated from the total carbon consumption rate:

$$\frac{\partial X_s}{\partial t}=-\frac{M_C}{\rho_C}\mathbf{v}_C\mathbf{R} \tag{31}$$

in which M_C and ρ_C are the molecular weight and density of the char, respectively. The stoichiometric coefficient vector is given as $\mathbf{v}_C=[-1\ 0\ -1]$. It is assumed that the density of the solid phase remains constant regardless of the char conversion and the porosity is thus a unique function of conversion:

$$\Phi(X_s)=\Phi_0+(1-\Phi_0)X_s \tag{32}$$

In this model, the pores are assumed to be cylinders with axis direction normal to the particle surface. Since the porosity and specific surface area are the total volume and inner surface area of all pores, respectively, the local mean pore diameter can be determined from the surface area and porosity of the char:

$$d_p=\frac{4\Phi(X_s)}{S(X_s)}=\frac{4[\Phi_0+(1-\Phi_0)X_s]}{S_0(1-X_s)\sqrt{1-\psi\ln(1-X_s)}} \tag{33}$$

With the gasification proceeding after a certain stage, the char particle shrinks and the apparent radius (r_a) of the char particle starts to reduce. This critical point corresponds to the process when local conversion at the particle outer surface causes fragmentation. In the model, the critical conversion point for the fragmentation (X_{cr}) is introduced in order to determine the dynamic of r_a. When the local conversion at the surface is below X_{cr}, the apparent radius remains unchanged but beyond X_{cr}, further conversion of char at the surface will cause shrinkage in the particle radius. Based on this consideration, the change in char

apparent radius with time can mathematically be expressed as

$$\frac{\partial r_a}{\partial t}=0 \quad \text{if } X_s(r_a)<X_{cr}, \qquad \frac{\partial r_a}{\partial t}=-\frac{\partial X_s(r_a)}{\partial t}\Big/\frac{\partial X_s(r_a)}{\partial r} \quad \text{if } X_s(r_a)\geq X_{cr} \tag{34}$$

2.6. Surface gas concentration

Gas concentration at the outer surface of the char particle is evaluated in order to provide boundary conditions for solving the proposed model. It is assumed that at the char surface the external convective mass transfer rate for the gas components to the surface must be equal to the transportation rate through the char particle surface (no accumulation at the surface), hence:

$$\mathbf{N}(r_a)=-\frac{\Phi}{\tau}\left([\mathbf{B}]^{-1}\frac{\partial \mathbf{C}}{\partial r}+\frac{RTB_0}{\mu}\frac{\partial}{\partial r}C_t[\mathbf{B}]^{-1}[\mathbf{A}]\mathbf{C}\right)\Big|_{r_a}=k_c[C_b-\mathbf{C}(r_a)] \tag{35}$$

where C_b is the component concentration in the bulk gas outside the char particle; k_c is the mass transfer coefficient which is determined from the correlation of forced convection mass transfer of a spherical particle (Baxter and Robinson, 2004):

$$k_c=\frac{ShD}{2r_a}; \quad Sh=2.0+0.552Re^{0.5}Sc^{1/3} \tag{36}$$

3. Numerical method for solving the developed model

In the developed model, gas species concentration ($\mathbf{C}$) and char conversion rate (X_s) are the objective variables to be determined. Since porosity is the function of conversion rate, Eq. (14) can be re-arranged as follows:

$$\frac{\partial \mathbf{C}}{\partial t}=\frac{(\partial(\Phi\mathbf{C})/\partial t)-\mathbf{C}(\partial\Phi/\partial t)}{\Phi}=\frac{(\partial(\Phi\mathbf{C})/\partial t)-\mathbf{C}(1-\Phi_0)(\partial X_s/\partial t)}{\Phi} \tag{37}$$

Since char particle apparent radius starts to reduce after the critical carbon conversion rate and will eventually approach zero, the moving boundary method is used in solving the proposed model (Ebahimi et al., 2008).

As the model involves a series of highly nonlinear, partial differential equations (PDEs), the model can only be solved using an appropriate numerical technique. In solving the model, the solid char particle is divided into N discrete nodes from the centre to the outer surface of the particle, and physical properties at each node are evaluated by the central difference method. The radius coordinate, r, is replaced by dimensionless spatial variable, s, therefore, the domain concerned is converted into expression of relative coordinate:

$$r=r_a\cdot s, \ \forall r\in[0,r_a]; \ \forall s\in[0,1]$$

Therefore, the derivative of variables represented by Y at all nodes is transformed from the original PDEs (Wang and Bhatia, 2001):

$$\left.\frac{\partial Y}{\partial t}\right|_s=\left.\frac{\partial Y}{\partial t}\right|_r-\frac{\partial Y}{\partial s}\frac{\partial s}{\partial r_a}\frac{\partial r_a}{\partial t} \tag{38}$$

where the variable s is defined as

$$\frac{\partial s}{\partial r_a}=-\frac{s}{r_a} \tag{39}$$

In order to obtain the numerical solution, the original PDEs were converted into a set of ordinary differential algebraic equations (DAEs), by converting the continuous variables into the discrete expression on N equal-space segments along the particle radius, thus the original six PDEs can be converted into 6N DAEs. In solving the model, different size of discrete nodes and different time steps have been tried to obtain converging and stable solutions using Matlab software. It has been found that the number of elements should be equal to, or greater than, 50 in order for the model to provide converging solutions at all possible input operating conditions.

The initial conditions can be established from the operational condition. At the start of the gasification process ($t=0$), gas compositions of the steam (H_2O) and three resultant gas species (H_2, CO and CO_2) are zero within the char particles ($C_1=C_2=C_3=C_4=0$). The composition of nitrogen (C_5) corresponding to atmospheric pressure and operating temperature can be calculated using the Ideal Gas Law. The solid char conversion at the start is zero ($X_s=0$).

The boundary conditions for the gaseous species at the char centre ($r=0$) and at the char surface ($r=r_a$) have been given in Eq. (6). Since there is no transportation of solid char occurring, the boundary condition for carbon conversion (X_s) is not needed.

The numerical scheme of solving the developed model can be described as four steps:

- Firstly, the time derivatives of deviation variables at a given radial position $(\partial Y/\partial t)|_r$, are evaluated from the differential equations by the central difference method.
- The moving boundary method is then used to transform the time derivatives of the deviation variables into a dimensionless form $(\partial Y/\partial t)|_s$.
- PDEs are desecrated into DAEs in order to obtain the numerical solution.
- Finally Matlab software, which employs mode15 method, is coded to integrate the DAEs for prediction of required values of gas species concentrations and carbon conversion rate.

The above procedures can be applied to both the gasification of biomass char and the gasification of coal char using corresponding microstructural properties such as area to volume ratio, pore structure parameter and porosity. For simulation of the gasification of blended biomass and coal char, a simple method of interpolating the solid material properties is used to quantify the blend properties.

4. Simulation results and discussion

4.1. Simulation results and comparison with experimental data

The developed model for the steam gasification of solid chars has been solved under the operating temperatures of 850, 900 and 950 °C as used in the experiments (Xu et al., in press). The input values for the simulations are given in Table 1 for biomass char and coal char, respectively. For simulation of blended biomass and coal chars, the properties of the biomass char and the coal char are linearly interpolated based on the proportion of each fuel in the blend char. The values of pre-exponential factors

Table 1
Input parameters and values in the model simulations.

Parameters	Description	Coal	Biomass
Ψ	Pore structure parameter of char	10	2
S_0	Initial specific area of char	13 000 m^2/m^3	200 000 m^2/m^3
Φ_0	Initial porosity of char	0.6	0.8
$k_{0,1}$	Pre-exponential factor of reaction 1	29 (s^{-1})	
$k_{0,3}$	Pre-exponential factor of reaction 3	4364 (s^{-1})	
$E_{A,1}$	Pre-exponential factor of reaction 1	175.84 kJ/mol	
$E_{A,3}$	Pre-exponential factor of reaction 3	248.12 kJ/mol	

and activation energy for reactions Eqs. (1) and (3) were obtained from literature (Souza and Marcio, 2004).

By using the input data given in Table 1, the developed model has been solved to predict gas production rates, product gas composition, and carbon consumption rate in steam gasification of pure biomass char, pure coal char and blended biomass and coal char. The simulated results for gasification of pure biomass char at 900 °C are shown in Fig. 2 for gas production rate and gas composition, and in Fig. 3 for carbon consumption rate. In the simulations, the heat-up stage is not included as the model does not include the heat transfer process. However, the heat-up stage is very short (about 2 min) compared to the complete gasification process (20 min or longer). The corresponding results for the gasification of coal char are shown in Figs. 4 and 5. In all of the figures, the experimental data are also presented for comparison with the model simulation results.

Comparison between simulation results and experimental data was also made for blended biomass and coal chars, and for different gasification temperature as used in the experiments (Xu et al., in press). The model simulation results are all in close agreement with the experimental data for the producer gas profile and overall carbon consumption rates. From the above comparison, confidence in the developed model has been gained and thus the model has further been applied to examine the effects of gasification temperature, char structure and blending ratio of biomass and coal. The results are presented as follows (where it is possible), experimental data are also included.

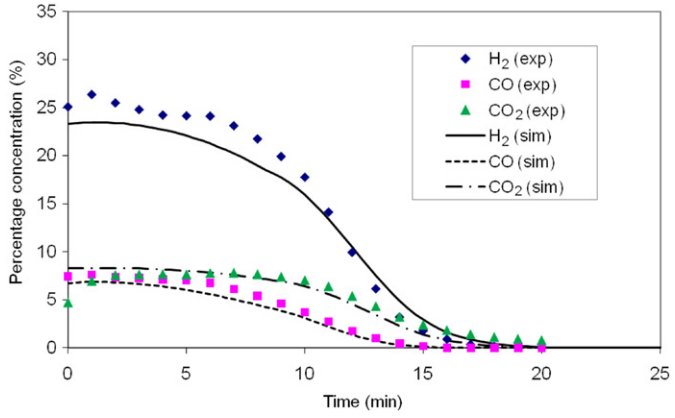

Fig. 2. Simulation and experimental results of gas production rate and gas composition in steam gasification of pure biomass char at 900 °C.

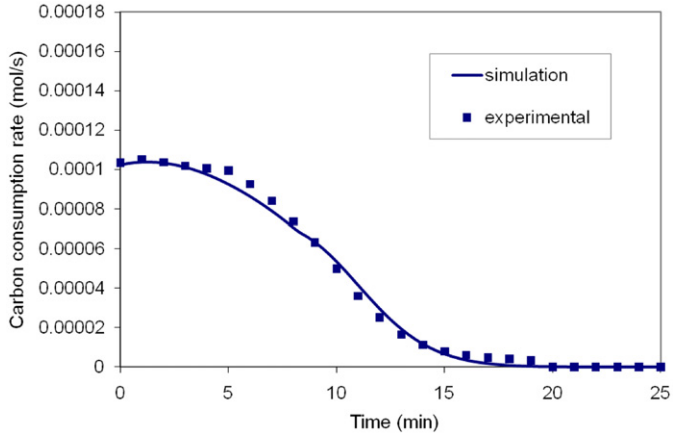

Fig. 3. Simulated and experimental results of carbon consumption rate for steam gasification of pure biomass char at 900 °C.

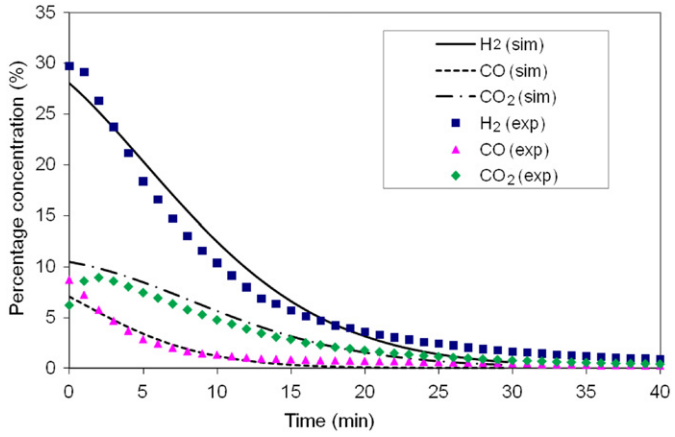

Fig. 4. Simulation and experimental results of gas production rate and gas composition in steam gasification of pure coal char at 900 °C.

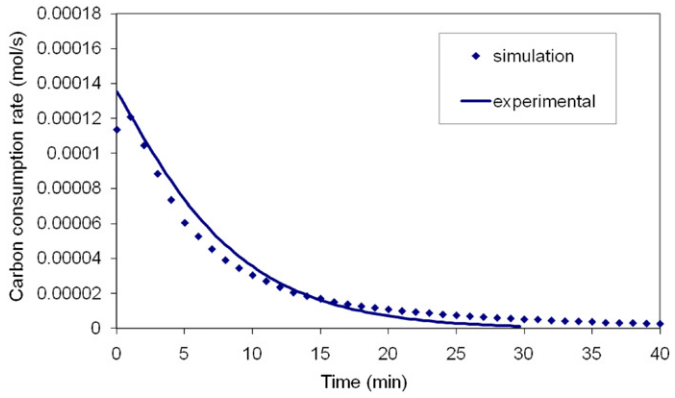

Fig. 5. Simulation and experimental results of carbon consumption rate for steam gasification of pure coal char at 900 °C.

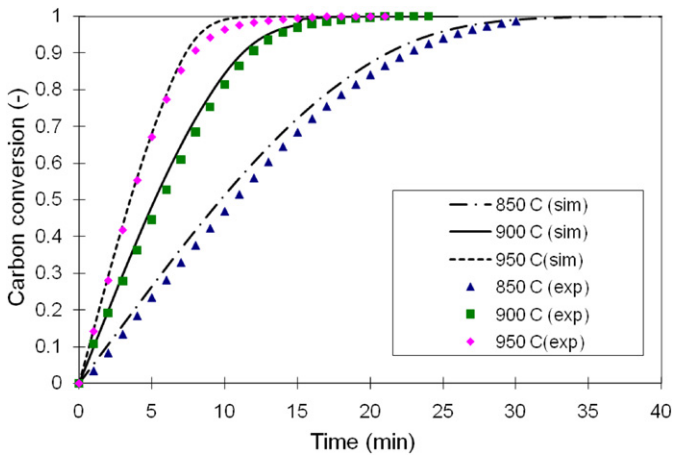

Fig. 6. Effect of gasification temperature on conversion dynamics of pure biomass chars.

4.2. *Effect of gasification temperature*

Figs. 6 and 7 show the simulation results and experimental data for carbon conversion in steam gasification of pure biomass char (Fig. 6) and pure coal char (Fig. 7) at three temperatures 850, 900 and 950 °C. The carbon conversion is the relative carbon consumed which is defined as the ratio of the carbon mass consumed in the gasification process to the initial carbon mass.

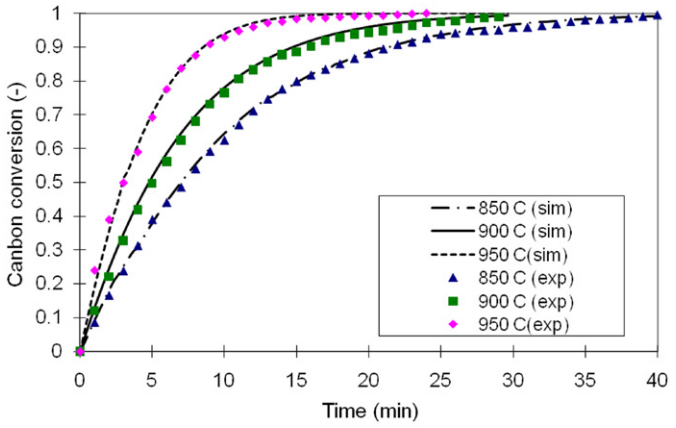

Fig. 7. Effect of gasification temperature on conversion dynamics of pure coal chars.

At the start of the gasification, the carbon conversion is zero as no carbon is consumed yet, but the carbon conversion approaches unity when the gasification is near completion when the majority of the carbon has been consumed.

From the conversion dynamic curves of biomass and coal, it is clearly seen that the gasification temperature enhanced the reaction rates for both types of chars. Furthermore, different reaction characteristics can be observed between the biomass char and the coal char. For the biomass char, the reaction rate remained approximately constant at the initial stage, indicated by the linear increase of the conversion dynamic curve. For the coal char, the exponential shape of the conversion dynamic curve indicates that the gasification reaction order is a first order reaction.

The close agreement between the model simulation and the experimental results further confirms the analysis of the gasification mechanism presented in the previous paper (Xu et al., in press). In gasification of the biomass char, the reactions mainly occur on and near the char particle surface thus constant reaction kinetics can be observed in the early stage of the gasification. However, in the late stage of the gasification, the surface becomes less and less, the reaction rates relative to the original char mass are reduced, resulting in a curved conversion curve. For the gasification of coal char, the reaction can occur in the micro-pores within the char particle due to the lower transfer resistance, therefore, the intrinsic reaction rates follow traditional first order kinetics.

Another interesting phenomenon observed is that increasing the temperature from 850 to 900 °C has a more significant impact in the gasification of biomass char than in the gasification of coal char. Further increase in the gasification temperature from 900 to 950 °C has more impact in the coal char gasification than in the biomass char gasification. Such phenomenon could be explained as the results of the competing effect of heterogeneous reactions and gaseous species diffusion within char matrix. Since biomass char has larger internal reactive surface area and smaller pore size compared with the coal char, the mass transportation within the char particle is the dominant factor for the biomass char gasification whereas for the coal char gasification, the intrinsic reaction are more important. As the temperature increases, the rate of mass transportation of gases is enhanced more significantly at the lower temperature range (850–900 °C). On the other hand, the intrinsic reaction rate can be increased more significantly at higher temperature range (900–950 °C). Therefore, the overall rate of biomass char conversion is more sensitive to the temperature increase at relatively lower temperature range but the gasification rate for the coal char is more sensitive to the higher temperature range.

4.3. Effect of microstructure of the solid chars

The overall specific reaction surface area (S) of the micro-pores in the char particle is one of the key parameters in the model which influences the char gasification process. This can be understood from its impacts on the gasification reaction rate and on the intra-particle transportation of the reaction species, referring to Eqs. (26) and (33). From Eq. (26), the reaction rate of heterogeneous reaction (R_j) is proportional to the specific reaction surface area, while Eq. (33) shows the mean pore diameter (d_p) is inversely proportional to the effective reaction surface area. For biomass char, which is more porous than coal char, the specific reaction surface area is greater thus the intrinsic reaction rate is higher compared to the coal char. However, the transportation of the gaseous species is also affected by the Knudsen Diffusivity effect which is the rate controlling factor of the overall diffusion due to the restriction of small pore diameter. Contrarily, for coal char with smaller specific reaction surface area, reaction rates are lower but the pore diameter is higher compared to the biomass char. Therefore, in the gasification of coal char, the reaction rate becomes the rate controlling factor.

Considering both the effect of intrinsic reaction rate and the overall transportation of gaseous species during the gasification process, in biomass char gasification the reactions on the char particle surface proceed faster than those in the micro-pores due to the greater resistance to gas transportation through the micro-pores. Therefore, the solid matter (carbon) on the surface layer of the biomass char will be consumed faster than that within the char particle. This can be clearly illustrated from the simulation results for biomass char gasification at 900 °C as shown in Fig. 8 in which the carbon conversion rate for three locations at the outer surface, at the middle location along the radius and in the centre of the char particle, is plotted as a function of elapsed time. The figure clearly shows the difference in the reaction rates along the radius resulting in a significant conversion gradient along the particle radius. It is also found that the surface shrinks in the gasification, which is indicated by shorter time of carbon conversion completion at the surface compared to the other parts within the biomass char particle.

On the other hand, the simulation results for the coal char gasification (Fig. 9) show that the conversion of the coal char is more uniform compared with the biomass char. Based on this finding, all the local conversion dynamics at different radial positions are very close to each other, indicating much less resistance for the reactant gas species to transfer within the char particles. Further analysis of the coal gasification process can reveal that the surface shrinkage is much slower than the biomass char gasification thus the overall reaction rate is slower than the

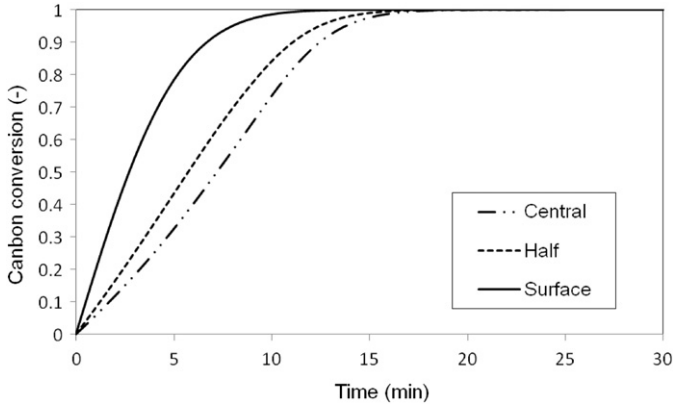

Fig. 8. Predicted conversion dynamics of biomass char at the char surface, mid-radius and in the char centre.

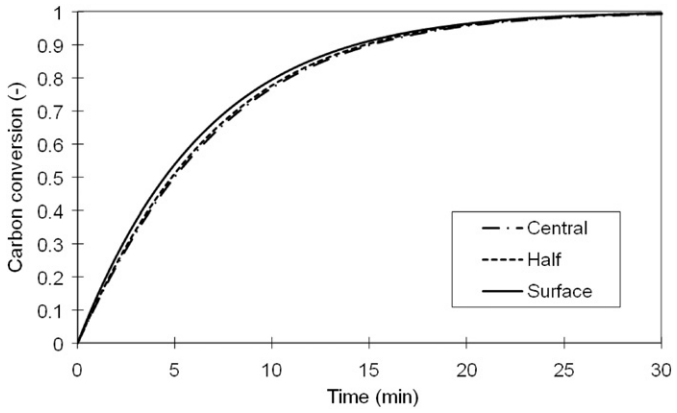

Fig. 9. Predicted conversion dynamics of coal char at the char surface, mid-radius and in the char centre.

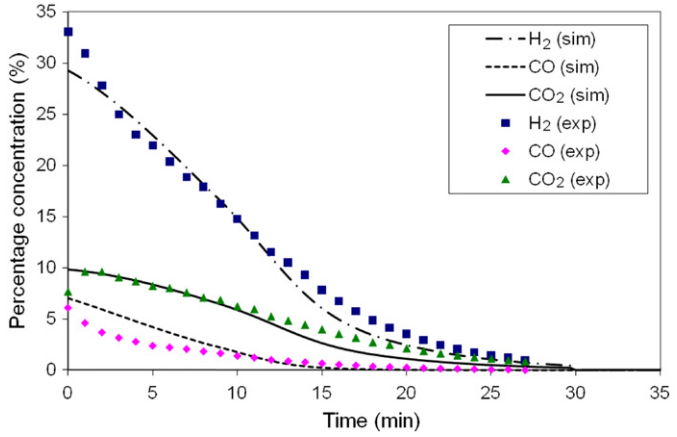

Fig. 10. Comparison of model simulated and measured results of gas production rate and gas composition in gasification of blend char with coal-to-biomass ratio of 20:80.

biomass char gasification. This can be confirmed by the longer gasification completion time at the same temperature compared to the biomass char gasification.

4.4. *Effect of biomass and coal blending*

The gasification process of blended biomass and coal chars has also been simulated using the developed model with the physical and chemical properties being determined based on the actual fractions of each solid in the blend char rather than on the blending ratio of the original materials. This is because the char yield of the coal is significantly higher than the biomass. In this work, the initial parameters such as surface area, porosity and density were also calculated based the actual fraction of each fuel in the blended char. The simulation results for gasification of blended chars with coal-to-biomass blending ratios of 20:80, 50:50, 80:20 are presented in Figs. 10, 12 and 14 for gas production profile and gas composition, and in Figs. 11, 13 and 15 for carbon consumption rate. In the figures, experimental data are also included for comparison with the simulation results and close agreements between the model simulation results and experimental data are observed.

The simulation results for the blended chars show that the gasification of blend chars is more likely to follow first order reaction kinetics without apparent constant reaction rate appearing in the early stage as observed in the gasification of pure biomass char (Figs. 2 and 3). This further confirms the findings

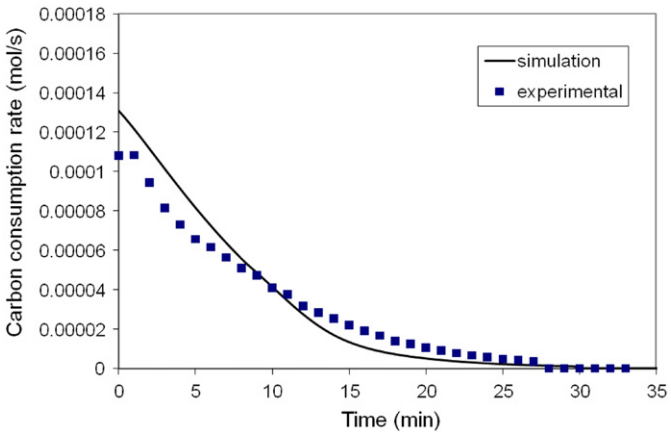

Fig. 11. Comparison of model simulated and measured result of carbon consumption rate in gasification of blend char with coal-to-biomass ratio of 20:80.

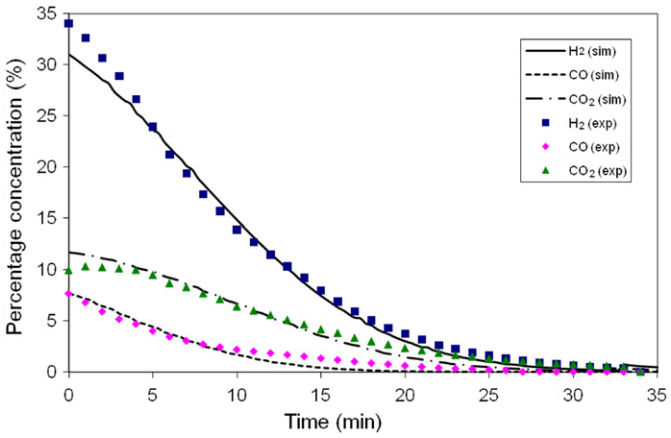

Fig. 12. Comparison of model simulated and measured results of gas production rate and gas composition in gasification of blend char with coal-to-biomass ratio of 50:50.

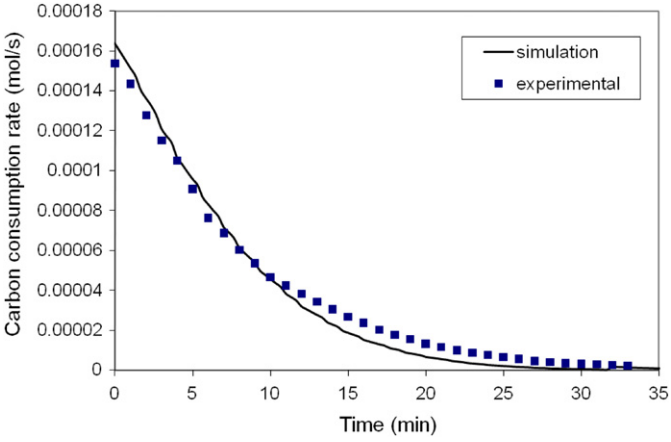

Fig. 13. Comparison of model simulated and measured results of carbon consumption rate in gasification of blend char with coal-to-biomass ratio of 50:50.

from the experiments (Xu et al., in press) that the characteristics of blend char gasification are more similar to those of pure coal chars (Figs. 4 and 5) which can be attributed to a number of factors. In the char generation, the biomass lost more volatile components than coal thus the actual char mass formed from the biomass was less than that from the coal. In addition, the microstructures between the pure biomass and coal are different,

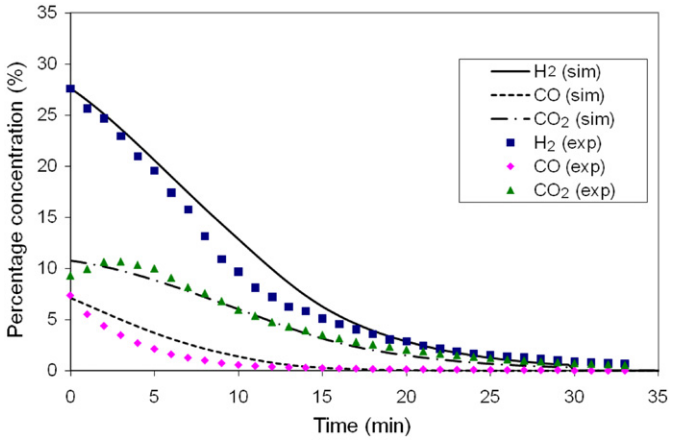

Fig. 14. Comparison of model simulated and measured results of gas production rate and gas composition in gasification of blend char with coal-to-biomass ratio of 80:20.

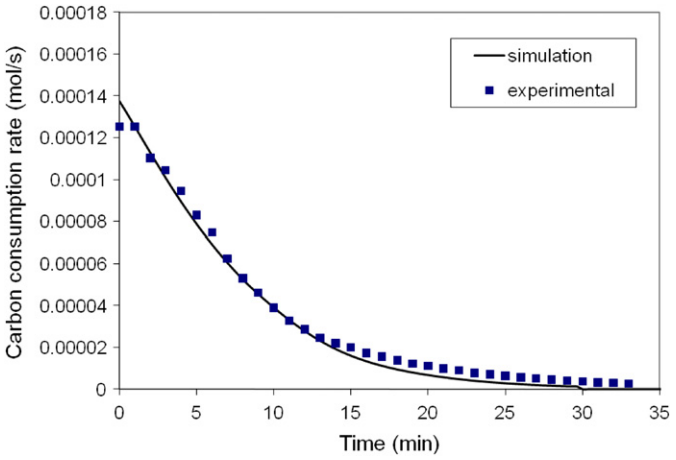

Fig. 15. Comparison of model simulated and measured result of carbon consumption rate in gasification of blend char with coal-to-biomass ratio of 80:20.

and the coal becomes more influential than the biomass when blended together.

5. Conclusions

In this work, a dynamic mathematical model has been developed for simulation of the steam gasification process of biomass char and coal char. This model is based on the reaction mechanism in the gasification, mass conservation and mass transfer as well as char structure characteristics. The reactions considered include: Steam-Gasification Reaction, Water–Gas Shift Reaction and Bouduard Reaction. The mass transfer process takes into account both diffusion and convective bulk flow of the reactant gas (steam), resultant gas species (H_2, CO, CO_2) and the carrier gas (N_2). The heat transfer is not included in the model since the particle size of the chars is very small and the Water–Gas Shift Reaction is exothermic thus the intra-particle temperature gradient is insignificant. The model has been solved using a numerical method to predict the gas production rate, gas composition and carbon consumption rate. In addition, the model can also predict the concentration distribution of gas species and carbon conversion rate along the char radial direction, from the centre to the outer surface of the particle.

The developed model is validated using experimental data and close agreement has been found between the model simulation results and the experimental data. The model simulation results show that the char structure (specific reaction surface area and micro-pore size) has significant impacts on both intrinsic reaction rate and the intra-particle mass transportation while the magnitude of these two competing processes determines the overall gasification process. The difference in the char structure is the key factor contributing to different gasification characteristics between biomass char and coal char.

The developed model is also applied to investigate the gasification of blended biomass and coal chars in which the solid material properties are interpolated based on the actual fraction of two fuels in the char. The close agreement between the modelled and experimental results suggests that the simple method to determine the blend properties is adequate for the simulation of gasification of the blend chars. The developed model presented in this paper will be employed to generate information which is used in a full scale gasifier model. The full scale gasifier is normally 2–10 MW for pilot or demonstration plants and is over 20 MW for full commercial plants.

References

Baxter, L.L., Robinson, A.L., 2004. Effects of intraparticle heat and mass transfer on biomass devolatilization: experimental results and model predictions. Energy and Fuels 18, 1021–1031.
Bhatia, S.K., 1987. Modeling the pore structure of coal. AIChE Journal 33 (10), 1707–1718.
Bhatia, S.K., Perlmutter, D.D., 1980. A random pore model for fluid–solid reactions: I. Isothermal, kinetic control. AIChE Journal 26, 379–386.
Biggs, M.J., Agarwal, P.K., 1997. The CO/CO_2 product ratio for a porous char particle within an incipiently fluidized bed: a numerical study. Chemical Engineering Science 52 (6), 941–952.
Ebahimi, A.A., Ebrahim, H.A., Hatam, M., Jamshidi, E., 2008. Finite element solution for gas-solid reactions: application to the moving boundary problems. Chemical Engineering Journal 144, 110–118.
Everson, R.C., Neomagus, H.W.J.P., Kasaini, H., Njapha, D., 2006. Reaction kinetics of pulverized coal-chars derived from inertinite-rich coal discards: gasification with carbon dioxide and steam. Fuel 85 (7–8), 1076–1082.
Fermoso, J., Arias, B., Pevida, C., Plaza, M.G., Pis, J.J., 2008. Kinetic models comparison for steam gasification of different nature fuel chars. Journal of Thermal Analysis and Calorimetry 91 (3), 779–786.
Gupta, P., Saha, R.K., 2003. Analysis of gas–solid noncatalytic reactions in porous particles: finite volume method. International Journal of Chemical Kinetics 36, 1–11.
Jackson, R., 1977. Transport in Porous Catalysts. Elsevier, Amsterdam.
Klose, W., Wolki, M., 2004. On the intrinsic reaction rate of biomass char gasification with carbon dioxide and steam. Fuel 84, 885–892.
Krishna, R., Wesselingh, J.A., 1997. The Maxwell–Stefan approach to mass transfer. Chemical Engineering Science 52, 861–911.
Lu, L., Kong, C., Sahajwalla, V., Harris, D., 2002. Char structural ordering during pyrolysis and combustion and its influence on char reactivity. Fuel 81, 1215–1225.
Marcio, L.S.S., 2004. Equipment and processes: Solid Fuels Combustion and Gasification: Modelling, Simulation, and Equipment Operation, 2nd ed.
Mastsumoto, K., Takeno, K., Ichinose, T., Ogi, T., Nakanishi, M., 2009. Gasification reaction kinetics on biomass char obtained as bu-product of gasification in an entrained-flow gasifier with steam and oxygenat 900–1000 °C. Fuel 88, 519–527.
Sadhukhan, A.K., Gupta, P., Saha, R.K., 2009. Characterization of porous structure of coal from a single devolatilized coal particle: coal combustion in a fluidized bed. Fuel Process Technology 90, 692–700.
Souza, S., Marcio, L.de, 2004. Solid Fuels Combustion and Gasification: Modeling, Simulation, and Equipment Operation. Marcel Dekker, New York.
Wang, F.Y., Bhatia, S.K., 2001. A generalized dynamic model for char particle gasification with structure evolution and peripheral fragmentation. Chemical Engineering Science 56, 3683–3697.
Welty, J.R., Wicks, C.E., Wilson, R.E., Rorrer, G., 1969. Fundamentals of Momentum, Heat and Mass Transfer, 4th ed.
White, F.M., 1991. Viscous Fluid Flow, 2nd ed.
Xu, Q., Pang, S., Levi, T. Reaction kinetics and producer gas compositions of steam gasification of coal and biomass blend chars, part 1: Experimental investigation. Chemical Engineering Science, in press, doi:10.1016/j.ces.2011.02.026.
Yamashita, T., Fujii, Y., Morozumi, Y., Aoki, H., Miura, T., 2006. Modeling of gasification and fragmentation behavior of char particles having complicated structures. Combustion and Flame 146, 85–94.